Available online at www.sciencedirect.com
SCIENCE DIRECT®
Journal of Magnetic Resonance 173 (2005) 288–295
JMR Journal of Magnetic Resonance
www.elsevier.com/locate/jmr

ESR spectrometer with a loop-gap resonator for cw and time resolved studies in a superconducting magnet

Ferenc Simon*,[1], Ferenc Murányi

Budapest University of Technology and Economics, Physics and Solids in Magnetic Fields Research Group of the Hungarian Academy of Sciences, P.O. Box 91, H-1521 Budapest, Hungary

Received 23 September 2004; revised 21 December 2004
Available online 29 January 2005

Abstract

The design and performance of an electron spin resonance spectrometer operating at 3 and 9 GHz microwave frequencies combined with a 9-T superconducting magnet are described. The probehead contains a compact two-loop, one gap resonator, and is inside the variable temperature insert of the magnet enabling measurements in the 0–9 T magnetic field and 1.5–400 K temperature range. The spectrometer allows studies on systems where resonance occurs at fields far above the $g \approx 2$ paramagnetic condition such as in antiferromagnets. The low quality factor of the resonator allows time resolved experiments such as, e.g., longitudinally detected ESR. We demonstrate the performance of the spectrometer on the $NaNiO_2$ antiferromagnet, the MgB_2 superconductor, and the RbC_{60} conducting alkaline fulleride polymer.

Keywords: cw ESR; Time resolved ESR; Longitudinally detected ESR; Loop gap resonators; Superconducting magnet; Alkaline fullerides; Superconductors; Strongly correlated spin systems

1. Introduction

Recent developments in electron spin resonance instrumentation aims at the use of high microwave frequencies and magnetic fields. This allows to obtain higher resolution and the study of magnetic field and microwave frequency-dependent phenomena [1–3]. Most spectrometers utilize a superconducting magnet with a resonant structure built in the bore providing high sensitivity, such as Fabry-Pérot [4–6] or cylindrical cavity resonators [7,8]. An alternative is to use the superconducting magnet in combination with a transmission configuration that enables temperature variability and multi-frequency operation at the cost of sensitivity [9,10]. Although, HF-ESR is seen to gain growing importance, the conventional low-field ESR experiments, such as X-band, are usually required to complement the spectroscopic information. It is often desired to perform the low-frequency experiments under similar experimental conditions than those at the high frequencies e.g. at low temperatures (down to 1.5 K) that is usually not available in commercial X-band spectrometers. A yet unexplored domain of the frequency-field diagram is the use of low microwave frequencies (<10 GHz) combined with high magnetic fields (6 T or higher). This would enable to obtain extra information on strongly correlated spin systems, e.g., antiferromagnets. In antiferromagnets with large exchange interaction and anisotropy, the so-called easy-axis resonance mode often appears at high magnetic fields and low frequencies [11]. The primary obstacle for the development of such spectrometers is the small usable size for a resonant microwave structure required for measurements in superconducting magnet bores. The recent developments of the NMR instrumentation beyond 1 GHz

* Corresponding author. Fax: +43 1 4277 51375.
E-mail address: fsimon@ap.univie.ac.at (F. Simon).
[1] Present address: Institut für Materialphysik, Universität Wien, Strudlhofgasse 4, A-1090, Wien, Austria.

1090-7807/$ - see front matter © 2005 Elsevier Inc. All rights reserved.
doi:10.1016/j.jmr.2005.01.002

enters the same domain with the same difficulties. A solution which satisfies all these requirements would be an X-band spectrometer combined with a superconducting magnet.

Here, we describe the development and performance of an ESR spectrometer that allows the use of low frequencies in the S- (2–4 GHz) and X- (8–12 GHz) bands and high magnetic fields (up to 9 T). A loop-gap resonator (LGR) with coaxial leads is placed inside the variable temperature insert of a superconducting magnet that is also used for high field/frequency ESR measurements with a transmission probehead. The LGR design is advantageous when lower cavity quality- and higher sample filling-factors are required such as for time resolved experiments for these microwave bands [12–16]. The instrument has two orders of magnitude lower sensitivity than a commercial ESP300 Bruker spectrometer that is compensated by the ~20 times larger usable samples providing comparable signal when sufficient sample amounts are available. The apparatus has comparable sensitivity as the transmission HF-ESR spectrometer and allows studies on the same samples. The special design of the LGR provides transparency for RF radiation ($f < 10$ MHz) and allows longitudinally detected ESR (LOD-ESR) measurements at S- and X-bands. LOD-ESR complements continuous wave (cw) ESR and spin-echo methods as it allows the measurement of short longitudinal relaxation times [17–19] and to separate overlapping ESR signals of spin species [20–23]. The instrument detects the modulation of the longitudinal magnetization, M_z, induced by a chopped microwave field, using a pick-up coil parallel to the external magnetic field, H_0. LOD-ESR spectrometers were previously built at X-band and we recently reported the development of the high-field version [19]. The performance of the apparatus in the cw-ESR mode is demonstrated on the $NaNiO_2$ antiferromagnet, on the MgB_2 superconductor below T_c [10] and in the LOD-ESR mode on the RbC_{60} conducting alkaline fulleride polymer [19].

2. The spectrometer

The block-diagram of the spectrometer operating in the cw-ESR mode including the optional LOD-ESR elements (dashed) is shown in Fig. 1. The microwave bridge is made of commercially available coaxial elements. The coaxial microwave circuit is connected to the probehead with a flexible coaxial cable (Pasternack Enterprises, PE3481) providing sufficient mechanical stability. The source is an Agilent (Agilent 83751B) synthesized frequency sweeper (2–20 GHz, maximal output power 20 dBm) that is locked to the microwave resonator (see below). The microwaves are directed toward the sample with a 4 port circulator (DITOM D4C2040 for 2–4 GHz and D4C8012 for 8–12 GHz) whose fourth port is terminated with a precision 50 Ω (Pasternack, PE6071). The circulator is placed 1 m apart horizontally and 0.5 m above the top of the cryostat, which provides stray magnetic fields below 0.5 mT at the circulator when the magnet is fully energized (8.9 T). The stray fields has no observable effect on the ESR spectra. The microwave loss is 1 dB for the 2–4 GHz band and 3 dB at 8–12 GHz for the exciting and the reflected signals. The broad-band microwave detector (Agilent 8474C, 0.01–33 GHz, sensitivity 500 mV/mW) does not require microwave bias thus we do not employ a reference microwave arm. This simplifies the operation and allows automatization during temperature sweeps when the microwave phase changes. This approach is customary in transmission high-field ESR instrumentation [3] and the correct microwave phase is obtained by using a sample as g-factor and microwave phase reference with a known line-shape (see below in detail). Our instrument allows both magnetic field and microwave amplitude modulated experiments. For the latter, we used the built-in option of the synthesized sweeper to produce an amplitude modulated output that was locked to a lock-in detector (Stanford Research Systems SRS830, 1 mHz–102 kHz). Magnetic field modulation is provided by a home-built, voltage controlled current source that is driven by the lock-in. The current source provides a constant modulation that is independent of the temperature-dependent impedance of the modulation coil.

The instrumentation of the LOD-ESR experiments closely follows the previous design of the HF-LOD-ESR apparatus [19] and here is only outlined. A coaxial PIN diode (Advanced Technical Materials, S1517D, 0.5-18 GHz bandwidth, switching speed: 10–90, 90–10%: 10 ns, insertion loss: 3 dB at 3 GHz and 5 dB at 9 GHz) provides the rapid microwave amplitude modulation and at X-band a TWT microwave amplifier (Varian, TWTA VZX-6980GZ, 8–12.4 GHz, maximum output 40 dBm, amplification 40 dB) is also built in. The PIN diode is driven by a high-frequency lock-in (Stanford Research Systems, SRS844, 0.025–200 MHz). An RF parasite component with the modulation frequency appearing on the output of the PIN diode is suppressed out with a band-pass microwave filter consisting of two facing waveguide to coaxial adapters (Agilent X281A). The LOD-ESR signal is detected with a longitudinal coil (see also below) that is part of an RF LC circuit. The capacitors are placed outside the magnet to prevent temperature drift of the RF resonance frequency. The LOD signal is amplified through a low noise RF preamplifier (Analog Modules 322-6-50, 200 Hz–100 MHz, gain 40 dB, input noise 380 $pV/\sqrt{Hz}$) and is phase sensitively detected by the SRS844 lock-in.

The spectrometer is based on a high homogeneity (10 ppm/cm) superconducting magnet (Oxford Instruments, 0–9 T) that is equipped with a variable tempera-

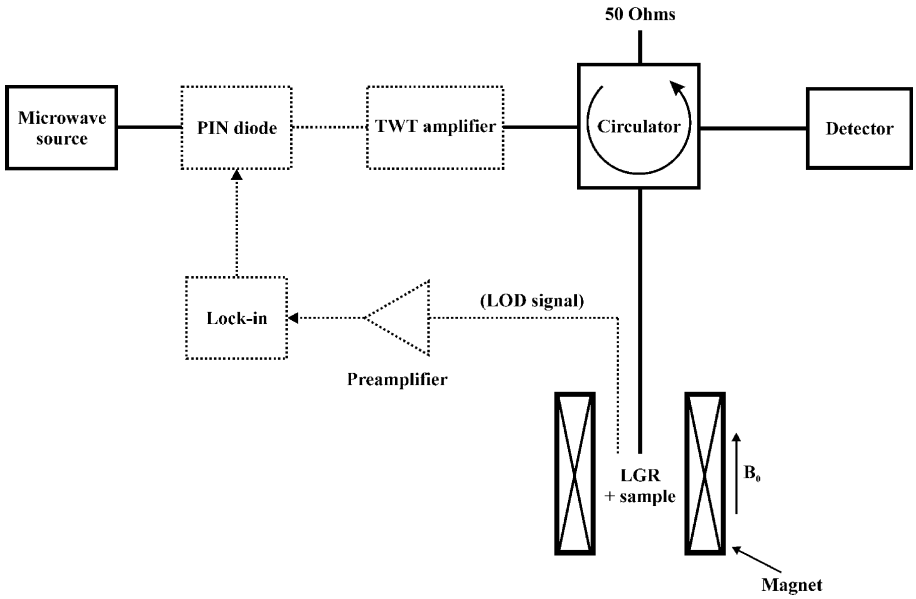

Fig. 1. Block diagram of the cw-ESR spectrometer with LGRs embedded in a superconducting magnet. The optional elements for the LOD-ESR measurements are shown in dashed boxes.

ture insert (VTI) for the 1.5–400 K temperature range and is regularly used for cw-HF-ESR measurements. Exchange gas in the sample compartment (40 mm internal diameter) thermally connects it to the VTI. Separation of the He gas in the sample compartment and the VTI avoids rapid He pressure changes inside the resonator when the cooling rate is modified. The outline of the probehead is shown in Fig. 2. Its outer diameter is 38 mm. Except the LGR itself, all elements are made of brass ($CuZn_{39}Pb_3$). The LGR (A) is placed between a lower (B1) and an upper (B2) microwave shield which are surrounded by a shielding cap (C). The shielding cap is a cylinder with a closed bottom and is fixed to the upper support (D) that is connected to the top of the magnet with two stainless steel tubes (not shown). Heating resistance is also attached to the upper support, the thermometer (Lakeshore, Cernox CX1050-SD) fixed to the LGR provides precise temperature monitoring of the sample. In cw-ESR mode, two coils (E1, E2) in an almost optimal Helmholtz configuration provide modulation with 0.6 mT/A. The coils are connected with a cable that is embedded in a brass tube (F) to prevent microphonics. The upper coil is connected to a semi-rigid coaxial cable above the D support with a short section of shielded flexible coaxial cable (not shown). We also use a pair of coils to detect the LOD RF signal in a quasi-Helmholtz configuration (see below). The shielded cabling guarantees shielding from the noisy environment, which is crucial for the LOD-ESR studies [19].

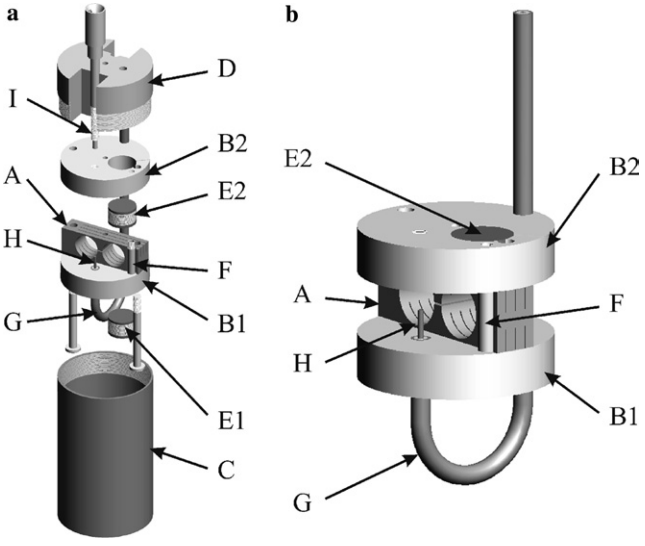

Fig. 2. (a) Split and (b) side views of the LGR probehead. A: LGR; B1, B2: lower and upper microwave shields; C: microwave shielding cap; D: upper support; E1, E2: modulation coils; F: tubing for modulation cable; G: curved semirigid cable section; H: coupling antenna; and I: coupling screw.

The microwaves are directed to the sample with a copper semi-rigid coaxial cable (Pasternack, PE3931) that is connected to a curved coaxial cable section (G) and ends in a capacitive antenna (H). Coupling is varied by a movable grounded screw (I) that is uniaxial with the antenna following [16]. The coupling screw is forced down vertically with the turning element, that is connected to the top of the cryostat (not shown), to maintain its good grounding. The capacitive coupling is of smaller size and provides enhanced mechanical stability as compared to the inductive one [16]. The fine adjustment of the coupling is performed by moving the coupling screw towards the antenna. On approaching the antenna, the coupling increases. However, the coupling

screw is only 3.8 mm apart from the LGR and its movement affects the resonance frequency. To minimize the required movement of the screw, the cavity is slightly undercoupled by adjusting the effective length of the antenna before inserting the probehead into the magnet. We found that magnetic fields up to 8.9 T have no observable effect either on the stability of the system or on the magnetic properties of the materials used.

The synthesized sweeper enables a simple design of the automatic frequency control (AFC) as it allows the frequency control through a DC feed-back signal and also AC modulation. Thus, the AFC involves an analogue lock-in (Stanford Research Systems SRS510) together with a simple circuit with passive elements only.

The LGRs for the different experiments are shown in Fig. 3. Figs. 3A and B show the resonators used for cw-ESR measurements at 3 GHz and for LOD-ESR measurements at 9 GHz, respectively. Similar LGRs were constructed for the 3 GHz LOD-ESR and 9 GHz cw-ESR (not shown). The dimensions of the LGRs together with the calculated and measured resonance frequencies and quality factors are summarized in Table 1. The

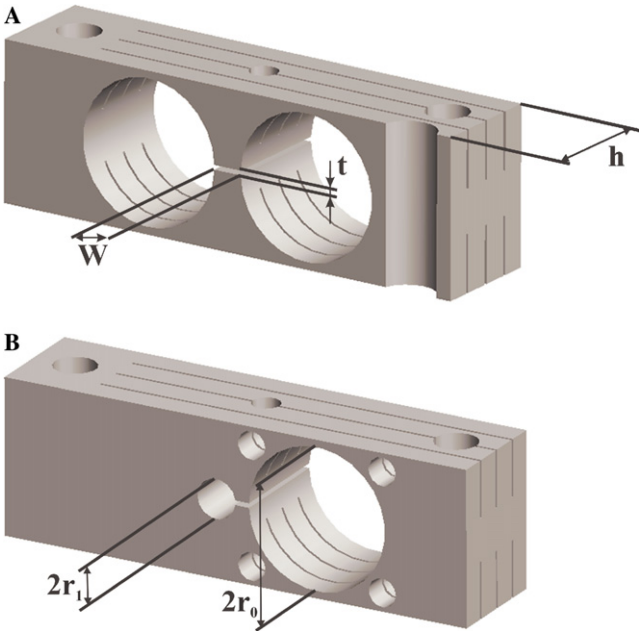

Fig. 3. (A) The LGR resonator operating in S-band for cw-ESR measurements, (B) the LGR working at X-band, optimized for LOD-ESR measurements.

LGR parameter notations are taken from [13] and are shown in Fig. 3. The calculated resonance frequency, ν_1, is obtained from the equivalent LC circuit using Eq. (2) in [13] and the resonant frequency with finite size corrections, ν_2, is calculated from Eq. (16) in [13]. The small space available for closing the flux inside the brass cap gives rise to a further ~10% frequency up-shift. The design allows the use of cylindrically shaped samples with diameters up to 8 mm and a height of 5–8 mm that are used for the transmission HF-ESR apparatus with 8 mm stainless steel tubing, such as a loose powder contained in a Teflon sample holder of a metallic sample as RbC_{60} [24] or fine grains of MgB_2 cast in epoxy [10]. Liquid samples can also be studied when placed inside Teflon sample holders.

The thin upper and lower walls of the LGR and the cuts perpendicular to the axis of the loops minimize eddy currents in the field modulation detected cw-ESR experiments. For LOD-ESR measurements, we use cavities made of the lower conducting brass to obtain better transparency for the detected RF signal. The pick-up coil is wound through the holes indicated in Fig. 3B in a quasi-Helmholtz configuration providing good transparency for the RF signal. The interaction between microwaves and the pick-up coil does not affect the pick-up signal. In the LOD-ESR mode, we have 12 dBm at 9 GHz and 16 dBm at 3 GHz at the sample. At 9 GHz, we can use a TWT amplifier (see Fig. 1) for the LOD-ESR measurements. The 4 port circulator limits the maximum power to 36 dBm peak or 33 dBm cw power. At low temperatures the power is limited to lower values.

3. Performance of the spectrometer

3.1. The cw-ESR spectrometer

One of the goals of the construction of the current spectrometer was to enable ESR studies at low microwave frequencies and high magnetic fields. In Fig. 4, the performance of our spectrometer is shown for such a combination on the $NaNiO_2$ material in its paramagnetic phase at $T = 25$ K. The sample was a powder that was placed in the same sample holder for both bands. The elements of the transmission Q-band spectrometer were described previously [19]. The spectra were

Table 1
Dimensions, resonant frequencies, and quality factors of the LGRs in this work

LGR (GHz)	r_0	r_1	W	t	h	ν_1	ν_2	ν_{EXP}	Q (copper)	Q (brass)
3	4.5	4.5	2	0.3	8	3.26	3.25	3.55	500	—
9	4.5	1.5	1	0.3	8	8.41	8.33	8.99	350	250

r_0 and r_1 are the radii of the sample and flux return loops, respectively, W is the width, t is the separation of the slit, h is the height of the LGR (all length parameters are in mm, frequencies in GHz units). Q is the quality factor of the critically coupled unloaded cavities.

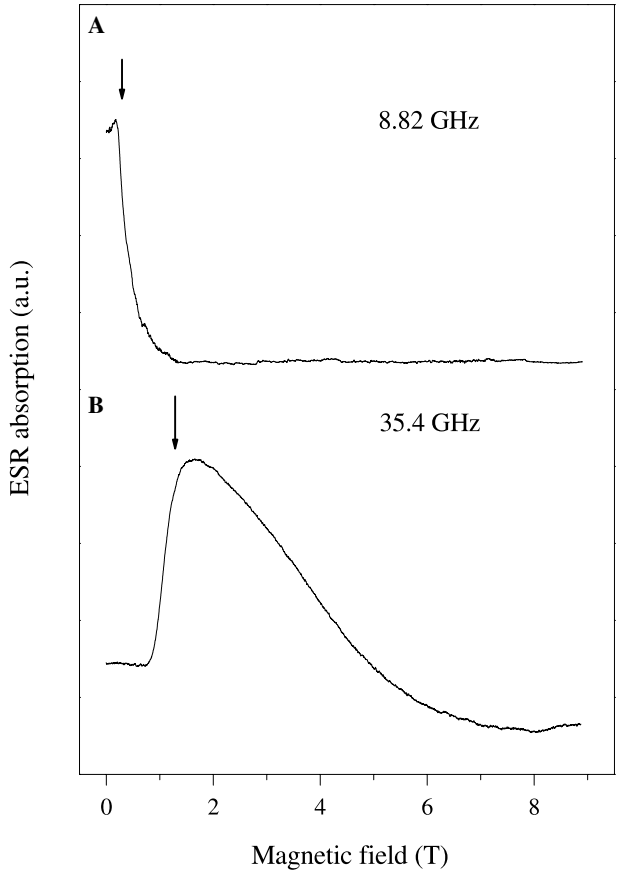

Fig. 4. The ESR absorption spectra of the $NaNiO_2$ material at $T = 25$ K in (A) X- and (B) Q-bands. The spectra were detected with amplitude modulation. The Q-band experiment shows a small magnetic field-dependent background that originates from the inox tube used for the transmission experiment.

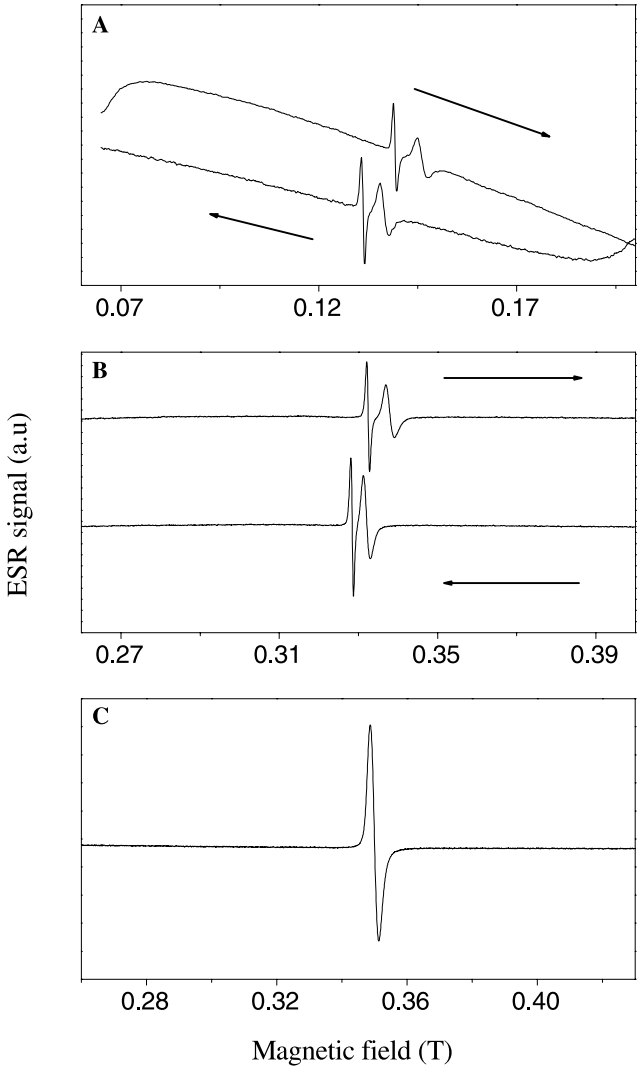

Fig. 5. MgB_2 spectra measured with the different spectrometers at 30 K. (A) Measured in the S-band LGR at 3.71 GHz, (B) measured in the X-band LGR at 9.14 GHz, and (C) measured in a Bruker ESP300 commercial spectrometer at 9.38 GHz. The narrow line at (A) and (B) is a KC_{60} for the field calibration, arrows indicate the field sweep direction. Note the significant hysteresis loop and the non-linear background in the S-band measurement due to the superconductivity in the sample.

recorded with amplitude modulation as the linewidth, ΔB, of the system is over 100 mT that exceeds our amplitude modulation limit of $B_{\mathrm{mod,max}} \approx 2$ mT. In this case, S/N is increased by $\Delta B/B_{\mathrm{mod\,max}}$ for amplitude modulation compared to magnetic field modulation, provided the noise originating from the non-resonant microwave reflections/absorptions, such as, e.g., magnetoresistance of the cavity, is smaller than the noise found for amplitude modulation. Although, no resonance absorption is observed for the material studied at high magnetic fields, Fig. 4 demonstrates the high stability of the spectrometer for such operations and the feasibility to perform low frequency, high magnetic field experiments.

In Fig. 5, we show typical magnetic field modulated cw-ESR spectra of MgB_2 in the superconducting state of this material. MgB_2 is a highly conducting material in its normal state and becomes a superconductor below $T_c = 39$ K [25]. The spectra were measured by the currently described spectrometer (A and B) at S- and X-band, respectively, as well as on a Bruker ESP300 commercial spectrometer at X-band (C). Irreversible effects of the superconducting diamagnetism give rise to a hysteretic background that is more pronounced in the lower-frequency measurements [27].

In the fine powder of the MgB_2 superconductor the conducting particles were separated by a powder of the non-magnetic SnO_2 insulator [10,26]. Measurement in the superconducting magnet requires a magnetic field calibrating g-factor standard. We used KC_{60} that has a narrow line with a temperature-independent intensity, lineshape and g-factor. It also serves as a microwave phase reference due to its well defined Lorentzian lineshape. Spectra of comparable quality can be obtained with the current LGR and the commercial spectrometers. The calculated sensitivity of the current spectrome-

ter is $S = 2 \times 10^{13}$ spin/G and $S = 5 \times 10^{12}$ spin/G for the S and X band LGRs, respectively. These values have to be compared to the $S = 5 \times 10^{10}$ spin/G of the ESP300 spectrometer determined on the same samples. The lower sensitivity can be partially compensated by the possibility of using up to 20 times larger amounts of the same sample without affecting the resonance mode of the cavity. As a result, we found that the current spectrometer provides only a factor 3–4 times smaller signal to noise ratios than the commercial apparatus when there is no limit on the sample availability. The sensitivity of the current LGR based spectrometer is two orders of magnitude larger than that of a transmission 24 GHz-superconducting magnet spectrometer [3] and is comparable to that of the transmission HF-ESR apparatus $S = 2 \times 10^{13}$ spin/G at 75 GHz (Jánossy et al., unpublished).

An advantage of the lower Q of the LGR is that it allows the detection of ESR in superconductors in magnetic fields as low as ~0.1 T as Fig. 5A demonstrates. The so-called vortex noise has been a limiting factor of field modulated ESR studies in superconductors using high Q commercial cavities that could be overcome only by avoiding magnetic field modulation [27]. Detailed temperature-dependent study of MgB_2 have been published separately [26].

3.2. The LOD-ESR spectrometer

In Fig. 6, we compare the performance of our spectrometer operating in the LOD mode with the previously developed 35 GHz transmission LOD-ESR apparatus [19]. We used RbC_{60} to calibrate and test the performance of our system. The LOD-ESR signal is proportional to the ESR saturation factor, $\gamma_e^2 B_1^2 T_1 T_2$, where γ_e, B_1, T_1, and T_2 are the electron gyromagnetic factor, exciting microwave field, longitudinal, and transversal relaxation times, respectively. Compared to the transmission ($Q = 1$) 35 and 75 GHz LOD-ESR spectrometers, a Q-fold increase in the signal is expected in the current spectrometer. The use of smaller magnetic fields reduces the longitudinal magnetization and the corresponding LOD signal. Altogether, one order of magnitude better performance is expected at the same power than with the 35 GHz spectrometer. However, we observed experimentally that the signal amplitudes are similar. The probable origin of the 10 times smaller sensitivity than expected is that the coil and microwave filling factors are smaller than for the 35 GHz LOD-ESR spectrometer. The quasi-Helmholtz configuration for the pick-up coils is known to have [28] a smaller filling factor than the solenoid used at 35 GHz [19]. The magnetic component of the microwave field inside the cavity is highly inhomogeneous and a substantial part of the sample is not in the maximum field position. This yields an experimentally determined $S = 7 \times 10^{16}$ spin/G$^{3/2}$ at

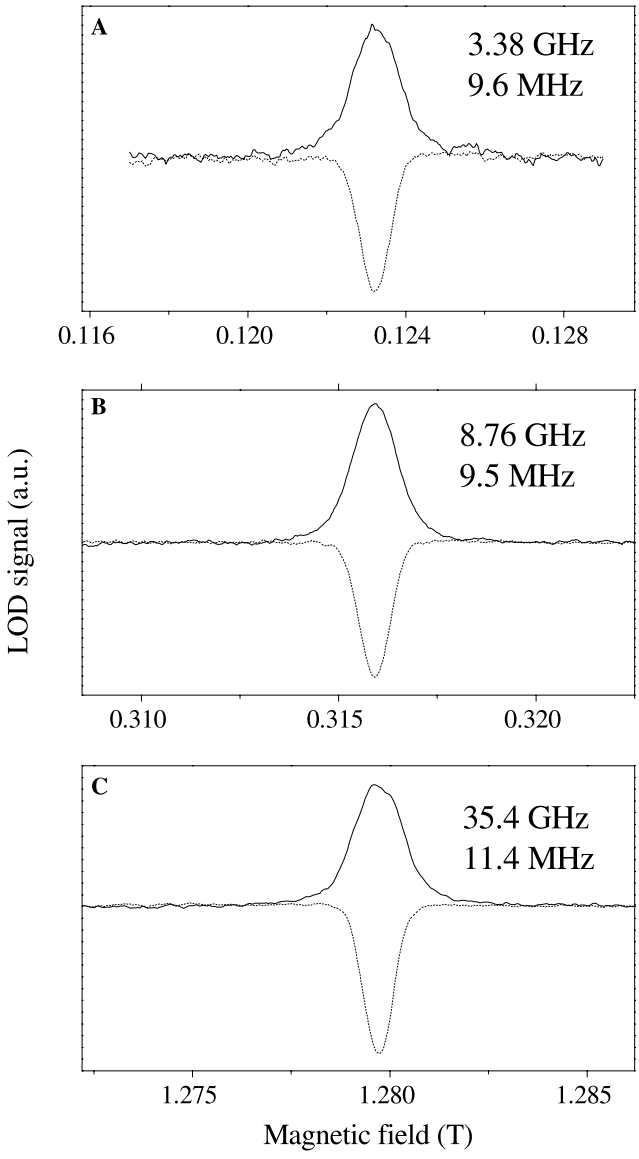

Fig. 6. Comparison of the LOD-ESR performance at several microwave frequencies, (A) S-band LGR, (B) X-band LGR, and (C) Q-band transmission [19] (solid and dashed lines are in and out-of-phase LOD signals, respectively). Note the larger linewidths of the in-phase signal that was explained in [19]. Insets show the microwave and the RF modulation frequencies.

3.5 GHz (16 dBm) and $S = 1.5 \times 10^{16}$ spin/G$^{3/2}$ at 9 GHz (at 12 dBm), this has to be compared to the 35 GHz transmission LOD-ESR that had $S = 3.3 \times 10^{16}$ spin/G$^{3/2}$ at 12 dBm [19]. At 9 GHz the TWT power amplifier at 33 dBm output power allows to achieve a maximum sensitivity of $S = 1.5 \times 10^{14}$ spin/G$^{3/2}$.

RbC_{60} has relaxation times in the 13–46 ns range that cannot be measured with usual spin-echo methods. On the other hand, LOD-ESR has been successful in determining T_1 in this compound [18,19]. The full method of obtaining T_1 data from the raw LOD-ESR data was reported previously [19] and is only outlined here. In the simplest case [18] when $\Omega \cdot T_1 < 1$, the ratio of the in

(u) and out-of phase (v) components of the oscillating longitudinal magnetization gives: $T_1 = \frac{1}{\Omega} v/u$. The accuracy of measuring T_1 relies not only on the magnitude of the detected LOD-ESR signal but also on the microwave amplitude modulation frequency, this latter being optimal when $\Omega \approx 1/T_1$. The maximum modulation frequency of our apparatus is limited to 10 MHz by the bandwidth of the LGRs used and the switching speed of the PIN diode. The best accuracy is for T_1 of 16 ns. However, T_1's down to 5 ns can still be measured with reduced accuracy.

4. Conclusion

In conclusion, we presented the construction and the performance of a spectrometer that utilizes low microwave frequencies and is placed inside the VTI of a superconducting magnet. The spectrometer is made of commercially available elements. It allows to obtain similar S/N as the commercial S- and X-band spectrometers on lossy samples, such as metals, when sufficient sample amounts are available. Thus, our system is an affordable alternative to the commercial low-frequency spectrometers and it can be readily installed at an HF-ESR laboratory. In addition, the system allows time resolved ESR experiments such as the detection of longitudinally detected ESR thus allowing the measurement of very short T_1's in metallic samples. The current spectrometer completes the previously developed 35 GHz version of LOD-ESR enabling magnetic field-dependent relaxation studies. We plan to perform experiments on systems where combination of low frequencies and high magnetic fields is required such as in antiferromagnets [29]. The approach reported here may also find applications in the emerging ultra high-field NMR applications as customary NMR frequencies approach the 1 GHz value [30] where our resonator design, completed with frequency tunability appears to be a feasible design.

Acknowledgments

This work is dedicated to the memory of László Berende. The authors would like to express their gratitude to A. Jánossy for helping the development of the current spectrometer and for many useful discussions. L. Forró is acknowledged for providing the RbC_{60} sample and for allowing the use of the ESP300 spectrometer. C. Petrovic, S. Bud'ko, and P. Canfield are acknowledged for the MgB_2 sample. S. de Brion is acknowledged for the $NaNiO_2$ sample. A. Sienkiewicz is gratefully acknowledged for suggesting the design of the resonator. B. Horváth is acknowledged for the technical assistance. Support from the Hungarian State Grants, OTKA T043255, OTKA TS040878, OTKA NDF45172, and FKFP 0352/1997 are acknowledged. F.S. acknowledges the Bolyai Hungarian Research Fellowship and the PATONN Marie-Curie MEIF-CT-2003-501099 grants for support and the hospitality of the University of Vienna during the preparation of the manuscript.

References

[1] G.R. Eaton, S.S. Eaton, High-field and high-frequency electron paramagnetic resonance instrumentation, Appl. Magn. Reson. 16 (1999) 159–160.
[2] J.H. Freed, New technologies in electron spin resonance, Ann. Rev. Phys. Chem. 51 (2000) 655–689.
[3] A.K. Hassan, L.A. Pardi, J. Krzystek, A. Sienkiewicz, P. Goy, M. Rohrer, L.C. Brunel, Ultrawide band multifrequency high-field EMR technique: a methodology for increasing spectroscopic information, J. Magn. Reson. 142 (2000) 300–312.
[4] E.J. Reijerse, P.J. van Dam, A.A.K. Klaassen, W.R. Hagen, P.J.M. van Bentum, G.M. Smith, Concepts in high-frequency EPR—applications to bio-inorganic systems, Appl. Magn. Reson. 14 (1998) 153–167.
[5] J.P. Barnes, J.H. Freed, A "shunt" Fabry-Perot resonator for high-frequency electron spin resonance utilizing a variable coupling scheme, Rev. Sci. Instrum. 69 (1998) 3022–3027.
[6] G.M. Smith, J.C.G. Lesurf, R.H. Mitchell, P.C. Riedi, Quasi-optical cw mm-wave electron spin resonance spectrometer, Rev. Sci. Instrum. 69 (1998) 3924–3937.
[7] J.A.J.M. Disselhorst, H. van der Meer, O.G. Poluektov, J. Schmidt, A pulsed EPR and ENDOR spectrometer operating at 95 GHz, J. Magn. Reson. A 115 (1995) 183–188.
[8] S. Hill, N.S. Dalal, J.S. Brooks, A multifrequency-resonator-based system for high-sensitivity high-field EPR investigations of small single crystals, Appl. Magn. Reson. 16 (1999) 237–245.
[9] F. Simon, A. Jánossy, F. Murányi, T. Fehér, H. Shimoda, Y. Iwasa, G. Baumgartner, L. Forró, Magnetic resonance in the antiferromagnetic and normal state of $NH_3K_3C_{60}$, Phys. Rev. B 61 (2000) 3826–3829.
[10] F. Simon, A. Jánossy, T. Fehér, F. Murányi, S. Garaj, L. Forró, C. Petrovic, S.L. Bud'ko, G. Lapertot, V.G. Kogan, P.C. Canfield, Anisotropy of superconducting MgB_2 as seen in electron spin resonance and magnetization data, Phys. Rev. Lett. 87 (2001) 047002–047005.
[11] S. Foner, in: G.T. Rado, H. Suhl (Eds.), Antiferromagnetic and Ferrimagnetic Resonance in Magnetism, vol. I, Academic, New York, 1963, p. 384.
[12] W. Froncisz, J.S. Hyde, The loop-gap resonator: a new microwave lumped circuit ESR sample structure, J. Magn. Res. 47 (1982) 515–521.
[13] W. Froncisz, T. Oles, J.S. Hyde, Q-band loop-gap resonator, Rev. Sci. Instrum. 57 (1986) 1095–1099.
[14] M. Willer, J. Forrer, J. Keller, S. Van Doorslaer, A. Schweiger, R. Schuhmann, Th. Weiland, S-band (2-4 GHz) pulse electron paramagnetic resonance spectrometer: construction, probe head design, and performance, Rev. Sci. Instrum. 71 (2000) 2807–2817.
[15] V. Weis, W. Mittelbach, J. Claus, K. Möbius, T. Prisner, Probehead with interchangeable tunable bridged loop-gap resonator for pulsed zero-field optically detected magnetic resonance experiments on photoexcited triplet states, Rev. Sci. Instrum. 68 (1997) 1980–1985.
[16] G. Elger, J.T. Törring, K. Möbius, Novel loop-gap probe head for time-resolved electron paramagnetic resonance at 9.5 GHz, Rev. Sci. Instrum. 69 (1998) 3637–3641.

[17] T. Strutz, A.M. Witowski, R.E.M. de Hekker, P. Wyder, Pick-up coil as a tool of measuring spin-lattice relaxation under electron spin resonance condition at high magnetic fields, Appl. Phys. Lett. 57 (1990) 831–833.
[18] V.A. Atsarkin, V.V. Demidov, G.A. Vasneva, Electron-spin-lattice relaxation in $GdBa_2Cu_3O_{6+x}$, Phys. Rev. B 52 (1995) 1290–1296.
[19] F. Murányi, F. Simon, F. Fülöp, A. Jánossy, A longitudinally detected high-field ESR spectrometer for the measurement of spin-lattice relaxation times, J. Magn. Res. 167 (2004) 221–227.
[20] J. Granwehr, A. Schweiger, Measurement of spin-lattice relaxation times with longitudinal detection, Appl. Magn. Res. 20 (2001) 137–150.
[21] J. Granwehr, J. Forrer, A. Schweiger, Longitudinally detected EPR: improved instrumentation and new pulse schemes, J. Magn. Res. 151 (2001) 78–84.
[22] G. Ablart, J. Pescia, S. Clement, J.P. Renard, Experimental evidence of two overlapping paramagnetic species, Solid State Commun. 45 (1983) 1027–1030.
[23] M. Martinelli, L. Pardi, C. Pinzini, S. Santucci, Dependence on relaxation times of longitudinally detected paramagnetic resonance, Solid State Commun. 17 (1975) 211–212.
[24] A. Jánossy, N. Nemes, T. Fehér, G. Oszlányi, G. Baumgartner, L. Forró, Antiferromagnetic resonance in the linear chain conducting polymers RbC_{60} and CsC_{60}, Phys. Rev. Lett. 79 (1997) 2718–2721.
[25] J. Nagamatsu, N. Nakagawa, T. Muranaka, Y. Zenitani, J. Akimitsu, Superconductivity at 39 K in magnesium diboride, Nature 410 (2001) 63–64.
[26] F. Simon, A. Jánossy, T. Fehér, F. Murányi, S. Garaj, L. Forró, C. Petrovic, S.L. Bud'ko, R.A. Ribeiro, P.C. Canfield, Magnetic field induced density of states in superconducting MgB_2: measurement of conduction electron spin-susceptibility. Available from: <cond-mat/0302620>.
[27] A. Jánossy, R. Chicault, Electron paramagnetic resonance without vortex noise in superconducting Gd doped YBaCuO, Physica C 192 (1992) 399–402.
[28] D.I. Hoult, R.E. Richards, The signal-to-noise ratio of the nuclear magnetic resonance experiment, J. Magn. Res. 24 (1976) 71–85.
[29] E. Chappel, M.D. Nunez-Regueiro, F. Dupont, G. Chouteau, C. Darie, A. Sulpice, Antiferromagnetic resonance and high magnetic field properties of $NaNiO_2$, Eur. Phys. J. B 17 (2000) 609–614.
[30] W.G. Clark, P. Vonlanthen, A. Goto, K.B. Tanaka, B. Alavi, W.G. Moulton, A. Reyes, P. Kuhns, Spin density wave order and fluctuations in $(TMTSF)_2PF_6$ at very high magnetic fields, Int. J. Mod. Phys. 16 (2002) 3252–3257.